



**MFP - A Calculation of Radiation Mean Free
Paths, Ionization and Internal Energies in Noble
Gases**

R.R. Peterson and G.A. Moses

May 1979

UWFDM-307

***FUSION TECHNOLOGY INSTITUTE
UNIVERSITY OF WISCONSIN
MADISON WISCONSIN***

**MFP - A Calculation of Radiation Mean Free
Paths, Ionization and Internal Energies in
Noble Gases**

R.R. Peterson and G.A. Moses

Fusion Technology Institute
University of Wisconsin
1500 Engineering Drive
Madison, WI 53706

<http://fti.neep.wisc.edu>

May 1979

UWFDM-307

Abstract

Noble gases are presently being considered in the protection of the first walls of particle beam and laser fusion reactors. When considering such protection schemes, one must have knowledge of the radiation transport properties, the ionization and the equations of state of the gas. We have developed a method of obtaining this information for a monatomic gas which uses simple physical models for the atomic processes in the gas. Photo-ionization, inverse Bremsstrahlung, Thomson scattering and atomic line absorption are considered as photon stopping mechanisms and the approximations used in studying these effects are described. Radiative recombination is assumed to be the only recombination mechanism so that the Saha equations for ionization are used. The errors induced by these approximations are deemed less important than the errors in the available atomic data. MFP, a computer code developed to calculate the radiation transport parameters, the internal energy and ionization of a gas, is described along with results for xenon and argon. This code allows dissimilar radiation and gas temperatures so that the radiation and gas need not be in equilibrium with each other. Results are discussed for temperatures between .4 eV and 500 eV and for densities between $2.7 \times 10^{14} \text{ cm}^{-3}$ and $2.7 \times 10^{22} \text{ cm}^{-3}$.

I. Introduction

Noble gases have been proposed as first wall protection for laser and particle beam fusion reactors.⁽¹⁾ For laser fusion applications a noble gas at a pressure of ~ 1 torr would minimize the chances of excessive beam losses due to scattering and gas breakdown while protecting the wall from X-rays and target debris. For particle beam reactors, a noble gas at a pressure of 50-300 torr would provide a medium for the establishment of a conducting channel for propagating the particle beam from the diode to the target. Damaging chemical activity between the wall and the buffer gases might also be avoided by the use of a noble gas.

Important problems with this method of first wall protection are possibly damaging shock waves and thermal radiation fluxes, which may propagate through the protecting gases. The large gas densities of particle beam reactors may impede the transport of thermal radiation to such a degree that a fireball is formed.⁽²⁾ In a fireball, the absorption of radiation becomes strong enough in the hot gas behind the shock wave that the mean free path of the radiation in the gas is much shorter than the characteristic length scale for changes in the density of the gas; that is, the gas behind the shock wave is optically thick. We are involved in calculations of the propagation of such a fireball and its effect on the first wall of a particle beam reactor.

Since the physics of fireballs is strongly influenced by the radiation transport in the gas, there is a need for the mean free paths of radiation. The internal energy and the ionization of the buffer gas are also important to fireballs. In this report we present a calculation of these quantities. A semi-classical model for the absorption of radiation through photo-

ionization and inverse Bremsstrahlung is used to calculate the radiation mean free paths as are series of approximations for the atomic line absorption. In calculating the ionization state of the gas the Saha model⁽⁴⁾ has been assumed. These models are discussed in more detail in section II. In section III we describe the computer code which we have developed to calculate these quantities. In section IV, we present results for the cases of argon and xenon with blackbody radiation temperatures and gas temperatures between .4 eV and 500 eV and for gas densities between $2.7 \times 10^{14} \text{ cm}^{-3}$ and $2.7 \times 10^{22} \text{ cm}^{-3}$.

II. Theory

We consider four radiative processes: photo-ionization, inverse Bremsstrahlung, Thomson scattering and atomic line absorption. For most cases, photo-ionization is the most important so that we consider it first. However, when the radiation temperature is low enough that most photons have energies less than the ionization energies of the most common ions, the other processes become important.

In this study we use the semi-classical model of the atom.⁽³⁾ In this model, the atomic electrons are assumed to travel in parabolic orbits and to occupy hydrogenic energy levels of principal quantum number n ,

$$E_n = \frac{-I(m)}{n^2}, \quad (1)$$

where $I(m)$ is the energy required to ionize the m^{th} electron. In this case, the cross section for photo-ionization of an atom in the $(m-1)^{\text{th}}$ ionization state is

$$\sigma_{\nu n} = \frac{64\pi^4}{3\sqrt{3}} \frac{e^{10} m_e(m)^4}{h^6 c \nu^3 h^5} \quad (2)$$

where $h\nu$ is the energy of the ionizing photon, c is the speed of light, m_e is the electronic mass and e is the electron charge. This cross section only holds when $h\nu \geq I(m)/n^2$ because the photon must have enough energy to move the electron out of the atomic well.

In Eq. (2), the Gaunt factor has been neglected because there are other unavoidable inaccuracies much larger than those accounted for with quantum mechanical corrections. These additional inaccuracies include deviations from classical orbits in the actual paths traversed by atomic electrons leading to a multiplicative change in Eq. (2), which could be accounted for with a Gaunt factor, and to a change in the frequency behavior of the cross section.⁽³⁾ Another error in our model for photo-ionization is in neglecting many-body effects; the core ion from which the electron is removed is not a single particle at a charge of m but is a collection of particles which all interact with the electron being ionized. These many-body effects are accounted for in the phenomenological ionization potential, $I(m)$. It has been claimed elsewhere that the deviations from non-classical orbits are not significant.⁽³⁾ Even for noble gases, determination of photo-ionization cross sections and ionization potentials is far from complete. The present state of research into the photo-ionization of noble gases is not completely satisfactory because, though fairly successful calculations have been completed⁽⁵⁾ using the phenomenological method of atomic pseudo-potentials, both Hartree-Fock and more sophisticated many-body calculations lead to significant deviations from the experimentally observed photo-ionization cross sections.⁽⁶⁾ In any case there are no accurately calculated or measured cross sections for photo-ionization or ionization potentials for highly ionized noble gases.

Acknowledging these unavoidable inaccuracies, we have used ionization potentials, $I(m)$, which have been extracted from a collection of experimental results⁽⁷⁾ and a set of values based on a simple calculation.⁽⁸⁾ These two sets of ionization potentials are shown for xenon in Fig. 1; we can

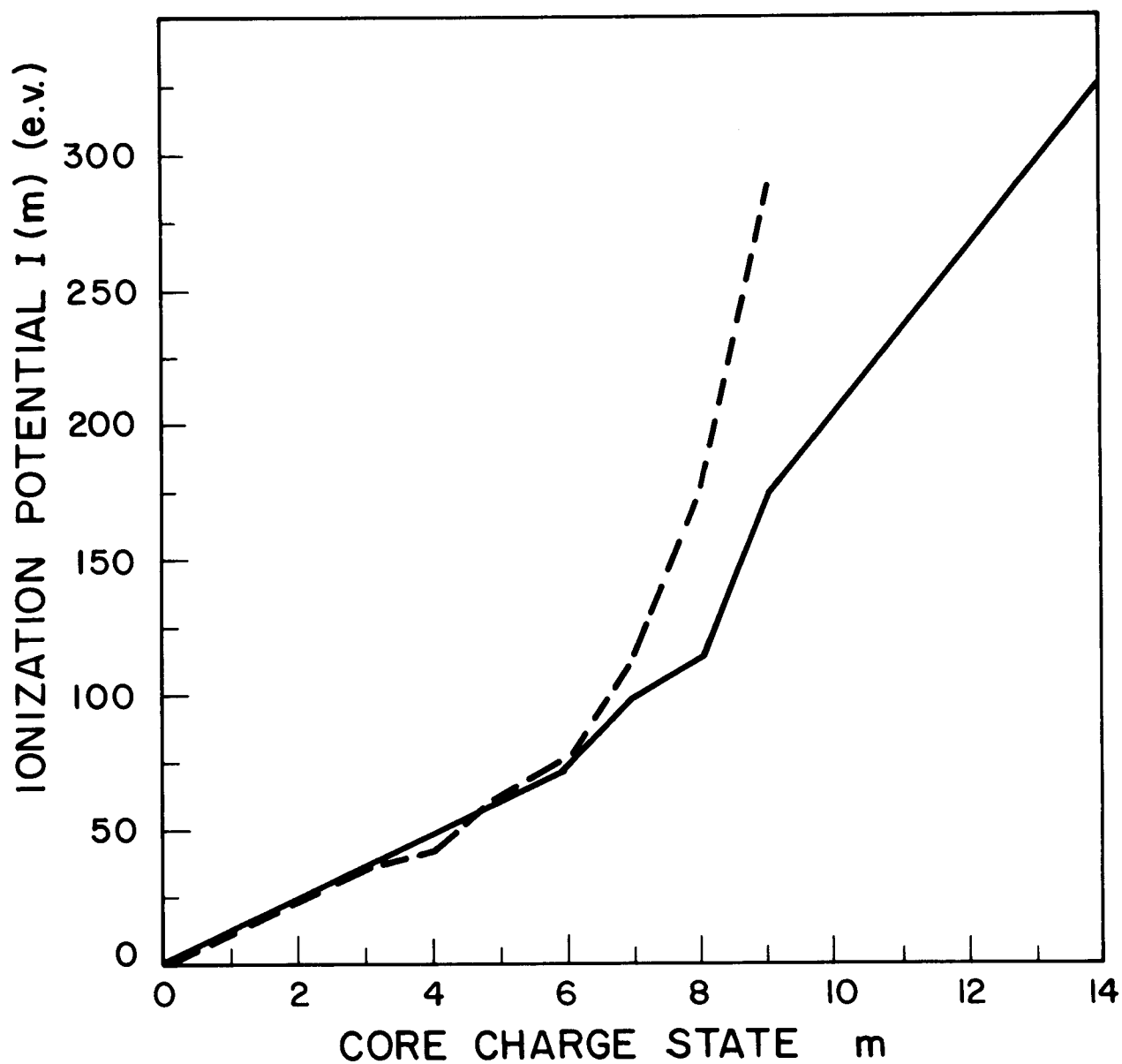


Figure 1 Ionization Potential for Xenon as Calculated by Carlson (solid line) and from a Variety of Measurements Compiled by Franklin (broken line)

only hope that the inaccuracies demonstrated in this figure will not significantly affect the transport of radiation through these gases. We feel that the adoption of the semi-classical model will cause less severe inaccuracies in the results than will the errors in the atomic parameters. Fig. 2 shows that theoretical ionization potentials for argon are in agreement with experiment.

From the cross section, Eq. 2, we may calculate the photo-ionization absorption coefficient for radiation at energy $h\nu$,

$$\kappa_{\nu}^i = \sum_m \sum_{n=n^*(m)}^{\infty} N_n^{(m)} \sigma_{\nu n}^{(m)} . \quad (3)$$

To conserve energy, n cannot be lower than $n^*(m)$, which is the principal quantum number of the lowest atomic level for which $h\nu > I(m)/n^2$. $N_n^{(m)}$ is the density of atoms in ionization state m and with an electron to be ionized having principal quantum number n . If

$$N > 10^{16} (T_p)^{7/2} \text{ cm}^{-3} ,$$

where N is the total density of gas atoms and T_p is the gas temperature in eV, then $N_n^{(m)}$ should be calculated in the Saha model where collisional three-body recombination is more important than radiative recombination.⁽⁹⁾ This is true for most of the cases we are interested in so that we can use the Saha equation to find the ionization state, m . We use Raizer's⁽⁴⁾ method of transforming the discrete m into a continuous variable, making $I(m)$ piecewise linear. This process is done such that $I(0)=0$ and $I(i)=I_i$, where I_i is the ionization potential of an atom which has sustained $i-1$ previous ionizations: examples of continuous $I(m)$'s are the lines in Figs.1 and 2.

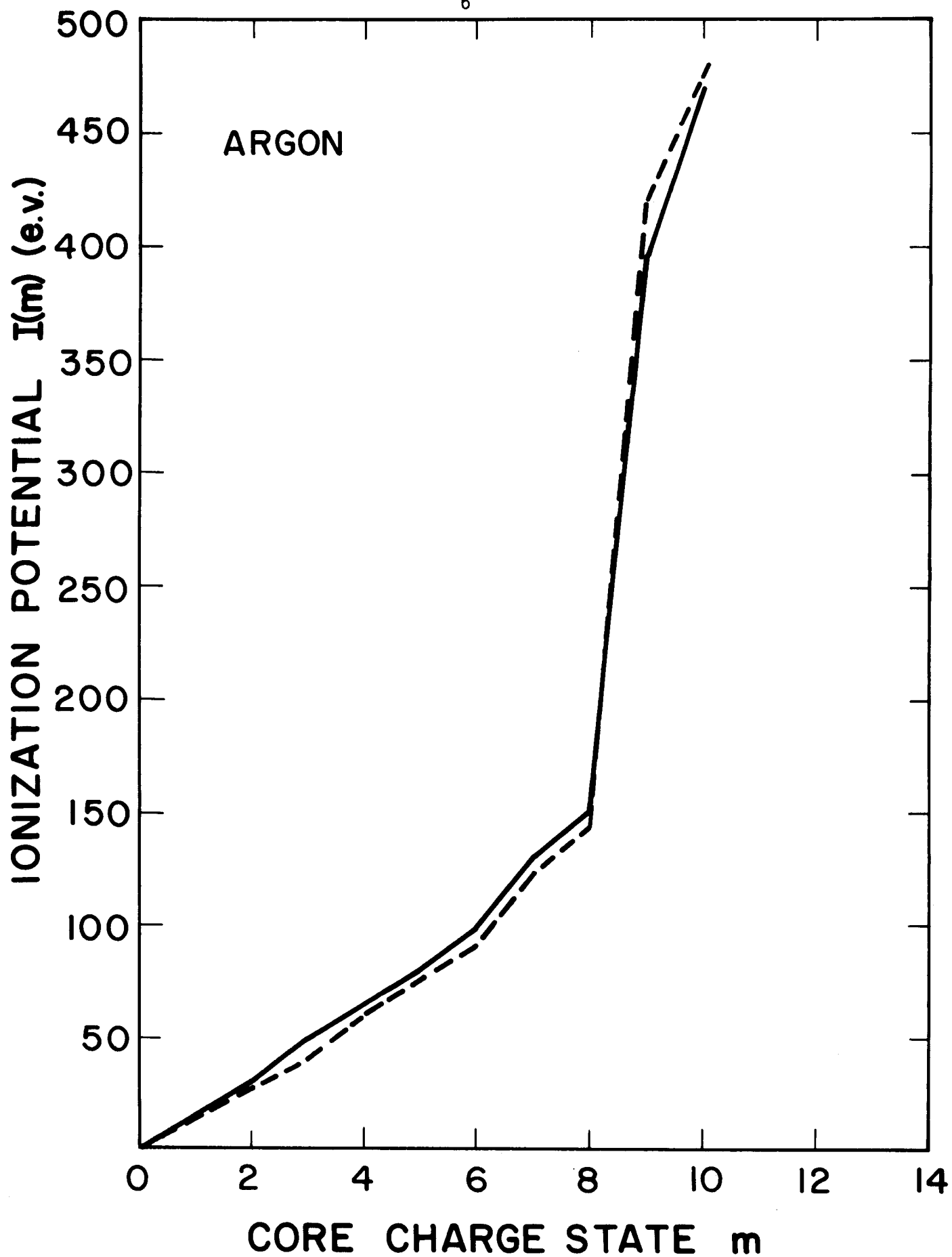


Figure 2 Ionization potential for argon as calculated by Carlson (solid line) and from a variety of measurements compiled by Franklin (broken line).

The mean ionization state, \bar{m} , is then the solution to the transcendental equation

$$I(\bar{m} + \frac{1}{2}) = T_p \ln \left(\frac{AT_p^{3/2}}{\bar{m}N} \right), \quad (4)$$

which is derived from the Saha equations,⁽⁴⁾ where $A = 6.04 \times 10^{21} \text{ eV}^{-3/2} \text{ cm}^{-3}$. Directly from the Saha equations, we may write down the ratio of the density of atoms in any ionization state $m+l$ to the density of atoms in charge state \bar{m} , where m is the largest integer less than \bar{m} :

$$\frac{N(m+l)}{N(\bar{m})} = \exp \left(- \sum_{i=1}^l \frac{|I(m+l) - I(\bar{m})|}{T_p} \right). \quad (5)$$

This equation, used in conjunction with the requirement that the total density is conserved, yields the density of atoms in charge state m , $N(m)$. By assuming that the atoms in each charge state are in thermal equilibrium at temperature T_p and that the atomic electrons fill hydrogenic energy levels, we relate $N_n(m)$ to the ground state density with the Boltzmann equation,

$$N_n(m) = N_1(m) \exp \left(\frac{-I(m)(1 - \frac{1}{n^2})}{T_p} \right). \quad (6)$$

In addition to photo-ionization, we have included inverse Bremsstrahlung as a photon absorption mechanism. We have included this because it is easily done and there is the possibility that it may be important when there are few electrons in atomic levels below the photon energy. The cross section for inverse Bremsstrahlung absorption is⁽³⁾

$$\sigma_{\text{vbrem}}^{(m)} = 2.4 \times 10^{-37} N_e m^2 / (h\nu)^3 \sqrt{T_p}, \quad (7)$$

where N_e is the electron density and $h\nu$ and T_p are in electron volts.

In considering Thomson scattering, we have assumed that all electrons, both bound and free, make the same contribution to the total Thomson cross section. For bound electrons when the photon energy is less than the ionization energy, the Thomson scattering cross section is actually larger than the Klein-Nishina cross section,⁽¹⁰⁾

$$\sigma_{\text{Thom}} = \left(\frac{e^2}{m_e c^2}\right)^2 \left\{ \frac{8\pi}{3} (1 - 2h\nu/m_e c^2 + \dots) \right\} . \quad (8)$$

This formula, valid only for $h\nu \ll m_e c^2$, neglects the coherent and incoherent photon scattering, which are important for tightly bound electrons and which increase the cross section.⁽¹¹⁾ Disregarding these effects and the frequency response of σ_{Thom} , the total Thomson scattering cross section per atom becomes

$$\sigma_{\text{sc}} = Z \left(\frac{e^2}{m_e c^2}\right)^2 \frac{8\pi}{3} . \quad (9)$$

It is well known that absorption lines can significantly influence the stopping of electromagnetic radiation in a gas.⁽¹²⁾ We have expressed the cross section for the absorption of a photon of energy $h\nu$ through an atomic transition from a state of principal quantum number n to a state of principal quantum number n' as

$$\sigma_{\text{line}}(n, n', \nu) = 2.78 \times 10^{-18} H(\nu, \nu_0, \Delta E) f_{nn'} \text{ cm}^2 , \quad (10)$$

where $f_{nn'}$ is the oscillation strength. We have used an approximation⁽³⁾ for $f_{nn'}$ of

$$f_{nn'} = \frac{32}{3\pi\sqrt{3}} \frac{1}{n^5} \frac{1}{n'^3} \frac{1}{\left(\frac{1}{n^2} - \frac{1}{n'^2}\right)^3} . \quad (11)$$

This represents an average of oscillator strengths for all of the possible transitions from states of principal quantum number n to states of principal quantum number n' : all of the permutations in values of the angular momentum quantum numbers ℓ and m have been accounted for as have the selection rules. This also assumes that the atomic levels are all hydrogenic.

$H(\nu, \nu_0, \Delta E)$ is a shape function in photon energy $h\nu$ for the atomic transition centered around energy $h\nu_0$ where

$$h\nu_0 = I(m) \left(\frac{1}{n^2} - \frac{1}{n'^2} \right) . \quad (12)$$

We pick H as a Gaussian with width ΔE and normalized so that its integral over photon energy is unity;

$$H(\nu, \nu_0, \Delta E) = \frac{282}{\Delta E} \exp \left\{ -\frac{(h\nu - h\nu_0)^2}{2(\Delta E)^2} \right\} . \quad (13)$$

ΔE is the line width of a bound-bound atomic transition. The most important source of line broadening is collisional or pressure broadening. Pressure broadening is due to shifts in the energy levels of absorbing atoms caused by the atomic field perturbing collisions between atoms. If the time it takes the collision to be completed is much less than the time it takes the fourier transform of the absorption spectral function to change, then line broadening

may be treated in the "Impact Approximation".⁽¹³⁾ Since lower energy levels are more tightly bound to the atomic nucleus, it is valid to approximate that these states are unaffected by collisions; thus, when considering line absorption one must only deal with shifts in the energy of the final state. With these approximations, the absorption spectra function for an isolated line becomes

$$F(\omega) = \frac{1}{\pi} \frac{\omega_i \langle i | D | i \rangle}{(\omega - \omega_i - d_i)^2 + \omega_i^2}, \quad (14)$$

where the frequency shift is

$$d_i = \frac{1}{\hbar} \operatorname{Re}(\langle i | H | i \rangle) \quad (15)$$

and the line width is

$$\omega_i = -\frac{1}{\hbar} \operatorname{Im}(\langle i | H | i \rangle). \quad (16)$$

The operator D acts only on the upper states of transitions and replaces the dipole operator \vec{d} :

$$\langle a | D | b \rangle = \sum_{\alpha} \langle a | \vec{d} | \alpha \rangle \langle \alpha | \vec{d} | b \rangle, \quad (17)$$

where $\langle a |$ and $| b \rangle$ are upper states in a transition and $| \alpha \rangle$ is a lower state.

The interaction Hamiltonian is

$$H = -i\hbar N \int_0^{\infty} dv f(v) v \int_0^{\infty} 2\pi b db \int_0^{\infty} (1-S) dv, \quad (18)$$

where the S-matrix for collisions between atoms is

$$S = 1 + \frac{1}{i\hbar} \int_{-\infty}^{\infty} dx V(x) + \frac{1}{(i\hbar)^2} \int_{-\infty}^{\infty} dx \int_{-\infty}^x dy V(x) V(y) + \dots \quad (19)$$

and $f(v)$ is the distribution function for perturbing particles. Here the modified potential is $V = -\vec{d} \cdot \vec{E}$ in the interaction representation and averaged over the perturbing particle's wave packet. \vec{d} is the atomic electric dipole operator and \vec{E} is the field of the perturbing particle at the center of the absorbing atom.

As the calculation is now done, this formalism has not been used for the line widths; but a reasonable line width is chosen as an input parameter. This formalism has been included at this point so that the complexity of the calculation can be appreciated. A future refinement of our calculations could include a calculation of the line widths.

The total absorption coefficient is written as

$$\begin{aligned} \kappa_{\nu}'' = & \sum_m \sum_{n=n^*(m)}^{\infty} N_n(m) \sigma_{\nu n}(m) + N \sigma_{sc} \\ & + \sum_m \sigma_{\nu \text{ brem}}(m) N(m) \\ & + \sum_m \sum_{n=n^*(m)}^{\infty} N_n(m) \sum_{n'=n+1}^{\infty} \sigma_{\text{line}}(n, n', \nu) . \end{aligned} \quad (20)$$

An example of such a calculation of the absorption coefficient is depicted in Fig. 3 for argon at $T_p = 1$ eV and $N = 10^{18} \text{ cm}^{-3}$. The absorption coefficient increases sharply as the photon energy rises through I_1 , $I_1/4$ and $I_1/9$, where the photon has gained enough energy to ionize electrons in energy levels at these values. At this temperature and density, argon is essentially transparent

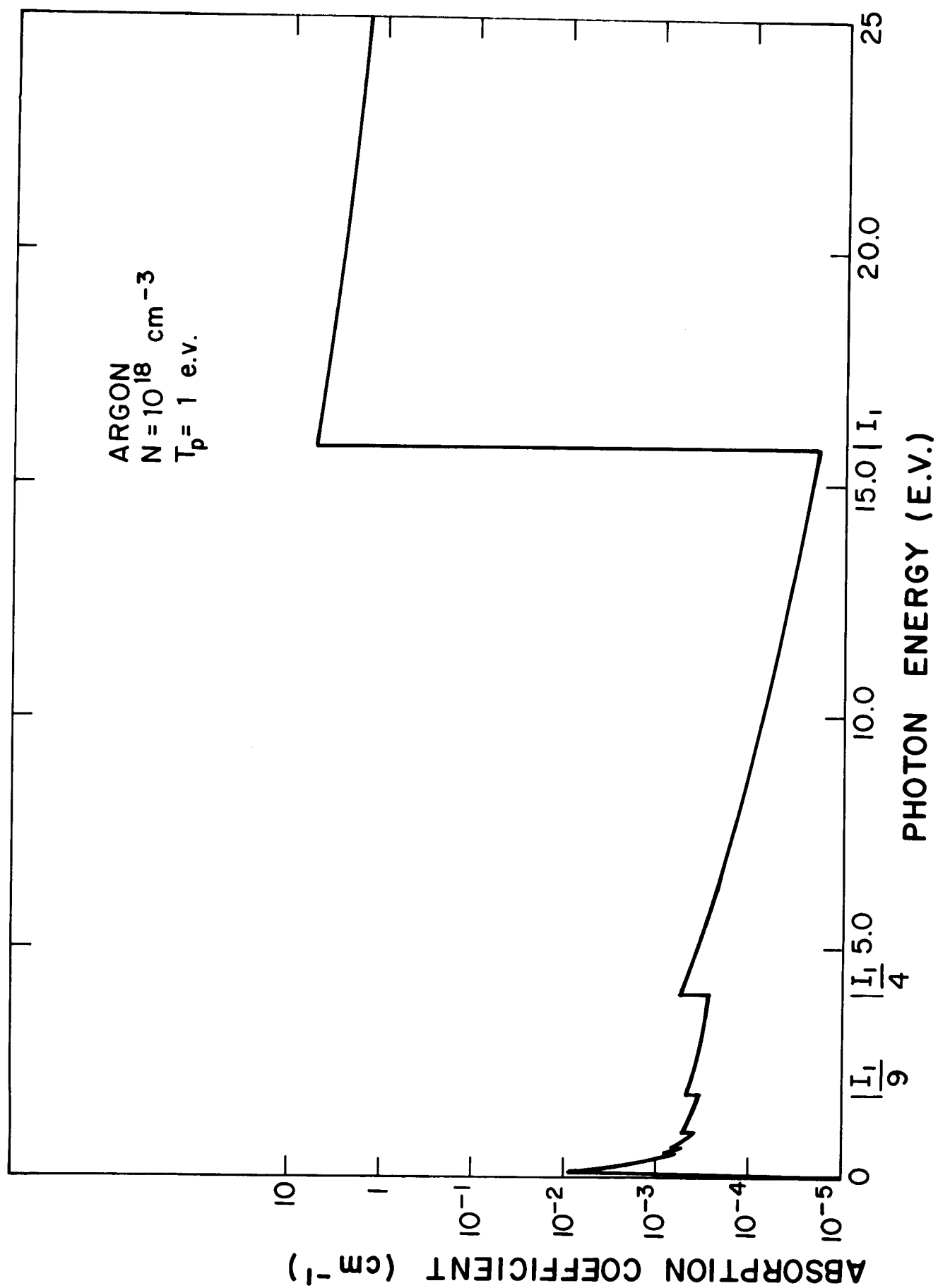


Figure 3 Absorption coefficient for argon. Highest three absorption edges are marked.

to radiation with photon energies less than 15.8 eV.

Knowing the absorption coefficient, we may calculate the mean free path of radiation in a gas. Any radiation field which is in thermal contact with some material body will not have its photons at one energy but will distribute them in energy. We assume that the radiation field is in equilibrium with some "blackbody" at temperature T_R , which need not be the temperature of the gas. This being the case, the photons are distributed in energy so that the spectral energy density is the Planck function,⁽¹⁴⁾

$$U_\nu = \frac{8\pi h\nu^3}{c^3} \frac{1}{\exp(h\nu/T_R) - 1} . \quad (21)$$

In a one-dimensional optically thick gas, there is approximately as much radiant energy flow in one direction as there is in its opposite direction, which allows us to use the diffusion approximation. The spectral intensity in one direction is found by integrating an isotropic radiant energy flux over a hemisphere of solid angle,

$$S_\nu = \frac{cU_\nu}{4} . \quad (22)$$

In the diffusion approximation⁽¹⁴⁾ this is

$$S_\nu = - \frac{c}{3\kappa_\nu} \vec{\nabla} U_\nu . \quad (23)$$

We integrate out the frequency dependence so that we can ultimately treat

the radiation field as a fluid which obeys the radiation diffusion equation,

$$\vec{S} = - \frac{\lambda c}{3} \vec{\nabla} U = \frac{\lambda c}{3} \vec{\nabla} \int dv U_v . \quad (24)$$

Here, λ is the Rosseland mean free path

$$\lambda \equiv \frac{\int_0^\infty \frac{1}{\kappa_v} (dU_v/dT_R) dv}{dU/dT_R} , \quad (25)$$

and \vec{S} is the frequency integrated energy flux density. A gas is optically thick when λ is less than the characteristic size of the gas.

When a one-dimensional gas is optically thin, most photons created in the gas will pass through the gas without being reabsorbed. Thus, the frequency integrated energy flux density is just proportional to the volume of the gas;

$$S \sim \frac{x c}{\lambda_1} U \quad (26)$$

where x is the characteristic width of the gas and λ_1 is the Planck mean free path,

$$\frac{1}{\lambda_1} \equiv \frac{\int \kappa_v U_v dv}{U} . \quad (27)$$

The forms of the Planck and Rosseland mean free paths differ because λ is calculated in an optically thick gas where the radiation is assumed to propagate by diffusion; the optically thin gas, in which λ_1 is the important value, lets the radiation free-stream through it.

The absorption coefficient used in Eqs. (25) and (27) should be corrected to account for induced emission. When electromagnetic radiation is present in matter, it is not only depleted by absorption but is replenished by spontaneous and induced emission. Spontaneous emission is dependent up to the state of the material and is unaffected by radiation already present in the system. The radiation present in the system does induce additional emission at the same frequency and in the same direction as its own. Since the induced emission is identical to the original radiation, it has the effect of reducing the absorption coefficient. **The effective** absorption coefficient becomes

$$\kappa_{\nu} = \kappa_{\nu}'' (1 - e^{-h\nu/T_R}) \quad (28)$$

and it becomes clear that induced emission only significantly reduces the effective absorption when the photon energies are less than the blackbody energy, T_R .

The internal energy of the gas is not that of an ideal gas because it must also include the effects of ionization of the gas. Ionization increases the energy of the i^{th} electron by I_i and increases the total electron thermal energy by increasing the density of free electrons. Thus, we may express the energy density of the gas as

$$E(T_p, N_p) = N_p \left[\frac{3}{2} (1 + \bar{m}) T_p + \sum_{i=0}^m I_i + (\bar{m} - m) I_{m+1} \right] . \quad (29)$$

III. Computer Code

We have developed a computer code which uses the model outlined in section II to calculate the radiation mean free paths, the ionization states and the internal energy of noble gases.

This code, which is written in Univac FORTRAN V, generates disk files containing tables of $\kappa(T_p, T_R, N_p)$, $\kappa_1(T_p, T_R, N_p)$, $\bar{m}(T_p, N_p)$ and $E(T_p, N_p)$ which are convenient for use in other codes. When used on the Univac 1110 computer at the Academic Computing Center of the University of Wisconsin-Madison, this code requires one second of CPU time for each choice of T_p , T_R , and N_p and 28,000 36-bit words of fast memory.

Fig. 4 is a flow chart for this code, which is called MFP. All of the real variables and arrays used in this code are double precision, with the exception of the arrays which are output to the disk which are single precision. We now briefly describe the variables, common blocks, subroutines, input and output for MFP.

Primary Variables

Here we list the important arrays and variables used in MFP.

| | |
|---------|--|
| ABSCN | Total absorption coefficient |
| D | Gas density |
| ELDEN | Electron density |
| END(10) | End points of mean free path integrals |

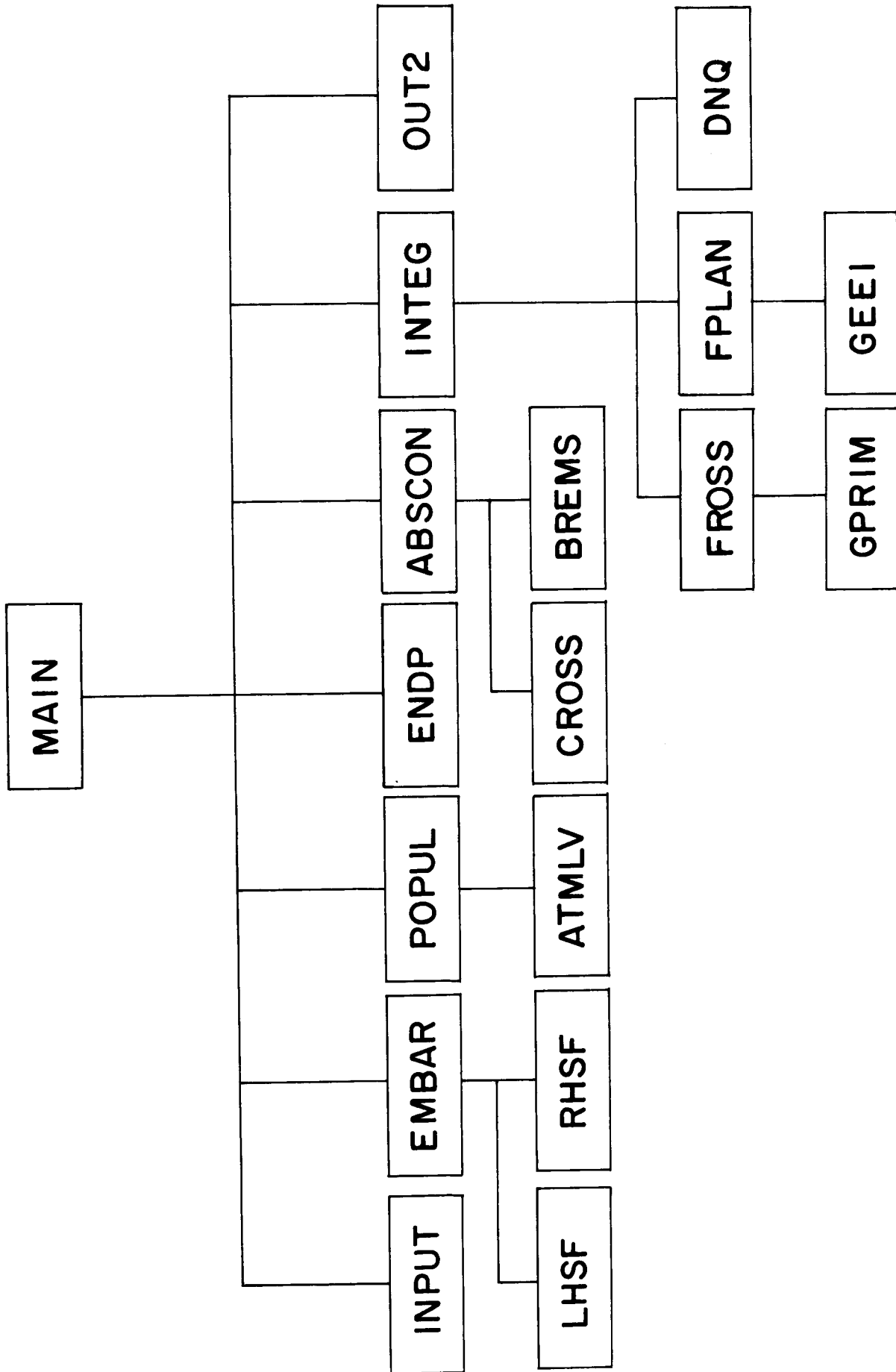


Figure 4 Flow chart for MFP.

| | |
|----------------|---|
| DELEI | Inverse width of bound-bound line |
| ERAD | Photon energy |
| FNN | Oscillator strength |
| G | Weighting function in Rosseland mean free path integration |
| G1 | Weighting function in Planck mean free path integration |
| H1 | Bound-bound line shape |
| IM | Largest integer less than \bar{m} |
| IZEE | Atomic number of gas |
| KAPPA (300) | Absorption coefficient |
| LROSS | Rosseland mean free path |
| L1 | Planck mean free path |
| MBAR | Average ionization state, \bar{m} |
| MINM | One less than the minimum difference between m and \bar{m} |
| N(K) | Density of $IM-MINM+K-1$ ionized atoms |
| NSUBN(K,NPRIN) | Density of atoms with $IM-MINM+K$ ionization electron in the NPRIN atomic level |
| POT(m) | Energy required to ionize the m^{th} electron |
| SIGBR | Free-free (Bremsstrahlung) cross section |
| SIGMA | Free-bound (photo-ionization) cross section |
| TP | Gas temperature |
| TR | Radiation black body temperature |

Output Variables

| | |
|------------|------------------|
| DENS(17) | Gas density |
| EEM(17,20) | Ionization state |

| | |
|-----------------|----------------------------------|
| EEN(17,20) | Internal energy |
| GL1(17,20,20) | Planck mean free path |
| GROSS(17,20,20) | Rosseland mean free path |
| TMPR(20) | Radiation black body temperature |
| TMPP(20) | Gas temperature |

Common Blocks

| | |
|--------|--|
| ABSORP | KAPPA(300) |
| COMEND | END(10), HIPT |
| CONTR | IPRT(20), JPO, JRO, IO, DELEI, EPSL, IMAX, JPMAX, JRMAX, DLOW, TLOW, DELTR, DELTP, DELD, UNFAC |
| POPU | IM, NSUBU(6,20), N(6), NMIN, ELDEN, D, MBAR |
| RITE | GROSS(17,20,20), GL1(17,20,20), DENS(17), TMPR(20), TMPP(20), EEM(17,20), EEN(17,20) |
| SAHDT | POT(55), STATE(55), IZEE, ATMAS |
| TEMP | TR, TP |

Main Program

The main program in this code is MAIN. It does no calculations itself but leads the code from accepting input through the calculations to the printing and storing of results. The mesh in radiation temperature - gas temperature - gas density space over which the results are spread is determined by parameters passed from subroutine INPUT in common block CONTR. The results are passed in common block RITE to subroutine OUT2, where they are printed and stored.

COMMON BLOCKS: CONTR, POPU, RITE, TEMP

SUBROUTINES CALLED: INPUT, EMBAR, POPUL, ENDP, ABSCON, INTEG, OUT2

Subroutines

ABSCON: This subroutine calculates the absorption coefficient for values of photon energy between 0 and HIPT. The values of photon energy are determined by end points received in common block COMEND from subroutine ENDP, where they are chosen to optimize the integrations in subroutine INTEG. Each of the eleven subintervals, given by the end points, are separated by EPSL and contain IPRT(2) points, except for the final subinterval which contains 2 IPRT(2) points. These two parameters, as well as HIPT, are passed from subroutine INPUT in common block CONTR. Photo-ionization, inverse Bremsstrahlung, atomic line absorption and Thomson scattering have been adopted as absorption mechanisms. The absorption coefficient is stored in KAPPA(300) and is passed in common block ABSORP for use in INTEG.

COMMON BLOCKS: ABSORP, COMEND, CONTR, POPU, SAHDT, TEMP

CALLED FROM: MAIN

SUBROUTINES CALLED: CROSS, BREMS

ATMLV(N,K,TP,KION,NATOM): This subroutine calculates the densities of atoms in atomic levels of the Bohr model. The atoms are assumed to be in equilibrium at temperature TP and in ionization state KION-1. These densities are used in ABSCON.

COMMON BLOCKS: SAHDT

CALLED FROM: POPUL

SUBROUTINES CALLED: None.

BREMS(ERAD,TP,IONST,ELDEN,SIGBR): This subroutine calculates the cross section for photon absorption through free-free transitions using the semi-classical approximation for atoms in the IONST charge state.

COMMON BLOCKS: None

CALLED FROM: ABSCON

SUBROUTINES CALLED: None.

CROSS(NPRIN, ERAD, KION, SIGMA): This subroutine provides the cross section for photo-ionization for use in subroutine ABSCON. The gas atoms being photo-ionized are in ionization state KION-1 and the electron being ionized is in an atomic energy level with a principal quantum number NPRIN. The ionizing photon has an energy of ERAD. The cross section, which is calculated in the semi-classical approximation, is passed as SIGMA.

COMMON BLOCKS: SAHDT

CALLED FROM: ABSCON

SUBROUTINES CALLED: None.

DNQ(H,DINP,DOUT,NDIM): This is a numerical quadrature routine that uses a simple trapezoidal rule. Prior to calling DNQ, the integrand must be evaluated at NDIM integration points, H being the distance between integration points, and stored in DINP(NDIM). The resulting values, integrated from the bottom end point up to each integration point, are returned in vector DOUT(NDIM).

COMMON BLOCKS: None

CALLED FROM: INTEG

SUBROUTINES CALLED: None.

EMBAR(ENER): This subroutine calculates the average ionization state of a gas by solving a continuous form of the Saha equation. This equation is transcendental and is solved by an iterative technique. This subroutine also calculates the internal energy of the gas and returns it as ENER.

COMMON BLOCKS: POPU, SAHDT, TEMP

CALLED FROM: MAIN

SUBROUTINES CALLED: LHSF, RHSF.

ENDP: To avoid discontinuities in κ_{ν} due to "K-edges", this routine is used to pick the end points of the integrations in photon energy used to calculate the radiation mean free paths. The integrations are to be broken into 10 smaller integrations where these shorter intervals have end points where the photon energies are equal to the first 5 atomic energy levels of the 2 most heavily populated ionization states.

COMMON BLOCKS: COMEND, CONTR, POPU, SAHDT

CALLED FROM: MAIN

SUBROUTINES CALLED: None.

FROSS(ERAD, ABSCN): This function is the integrand used in the integration over photon energy for calculation of the Rosseland mean free path.

COMMON BLOCKS: TEMP

CALLED FROM: INTEG

SUBROUTINES CALLED: GPRIM

FPLAN(ERAD, ABSCN): This function is the integrand used in the integration over photon energy for calculation of the Planck mean free path.

COMMON BLOCKS: TEMP

CALLED FROM: INTEG

SUBROUTINES CALLED: GEE1

GEE1(ERAD,G1): This subroutine calculates the Planck function used in the calculation of the Planck mean free path.

COMMON BLOCKS: TEMP

CALLED FROM: FPLAN

SUBROUTINES CALLED: None.

GPRIM (ERAD,G): This subroutine calculates the radiation temperature derivative of the Planck function to be used in the calculation of the Rosseland mean free path.

COMMON BLOCKS: TEMP

CALLED FROM: FROSS

SUBROUTINES CALLED: None.

INPUT: This subroutine reads atomic ionization potentials, sets the parameters necessary for computation and output and prints a heading which lists the initial parameter used. The ionization potentials are stored in POT(55) which is passed in common block SAHDT for use in other subroutines. The parameters needed for output and computation are passed to the other subroutines in common block CONTR. A sample output heading with the listed parameters is shown in Appendix A. A more complete description of the manner in which data may be read and parameters may be specified is given in the section on INPUT/OUTPUT.

COMMON BLOCKS: COMEND, CONTR, SAHDT

CALLED FROM: MAIN

SUBROUTINES CALLED: None.

INTEG(LROSS, L1): This subroutine sets up the integrations used to calculate the Rosseland and Planck mean free paths. Each of the integrations are broken into eleven subintegrals whose end points are received from subroutine ENDP through common block COMEND. Each of the subintervals consists of IPRT(2) points, where IPRT is a vector in common block CONTR which is set in subroutine INPUT. The subintervals are separated by EPSL, which is also received from INPUT through common block CONTR. The integrands are calculated by calling functions FROSS and FPLAN, respectively, for the Rosseland and Planck mean free paths. The absorption coefficient needed for these functions is passed from subroutine ABSCON in vector KAPPA which is in common block ABSORP. The integrations are achieved with calls to subroutine DNQ which does trapazoidal rule integrations.

COMMON BLOCKS: ABSORP, COMEND, CONTR

CALLED FROM: MAIN

SUBROUTINES CALLED: None.

LHSF(EM,II,LHS,IFLAG): This subroutine calculates one side of the continuous form of the Saha equation which in EMBAR is to be compared with the result of RHSF, the calculation of the right-hand side of the Saha equation. II and IFLAG are parameters used in EMBAR.

COMMON BLOCKS: SAHDT

CALLED FROM: EMBAR

SUBROUTINES CALLED: None.

OUT2: This subroutine prints and stores the results of this code. The results are passed in common block RITE from the main program. Even though the calculations have been done with double precision variables, the results are stored as single precision. Parameters controlling the printing and storing of results are contained in common block CONTR. A complete description of the form of the output is given in the INPUT/OUTPUT section of this report. A sample of the printed output is given in Appendix A.

COMMON BLOCKS: CONTR, RITE

CALLED FROM: MAIN

SUBROUTINES CALLED: None.

POPUL: This subroutine manages the calculation of the densities of atoms in various ionization states with electrons in various atomic states. Each of the atoms are assumed to be in one of the six ionization states which this subroutine chooses. With calls to ATMLV, this subroutine obtains and normalizes the atomic densities and then calculates the free electron densities.

COMMON BLOCKS: POPU, SAHDT, TEMP

CALLED FROM: MAIN

SUBROUTINES CALLED: ATMLV.

RHSF(D,TP,EM): This function is the right-hand side of the continuous Saha equation, which is compared with the results of LHSF in EMBAR.

COMMON BLOCKS: None

CALLED FROM: EMBAR

SUBROUTINES CALLED: None.

INPUT/OUTPUT

There are two types of input for this code: atomic ionization potentials and changes to the parameters which control the operation of the code. Both modes of input occur in subroutine INPUT.

Atomic ionization potentials are read into the matrix POT from unit 12. The ionization potentials are read, one piece of data per record, under a D 12.6 format. The number of records read is IZEE+1, which must be at least six, but under no circumstances will more than 55 records be read. There must be at least IZEE+1 or 55, whichever is smaller, records in unit 12. Input files for xenon and argon are shown as examples in Table I. This data must be written in double precision real.

The controlling parameters are first set to the default values in Table II. Parameters having no default values are IZEE and ATMAS, the atomic mass in grams. These must be set and any desired changes to the other parameters may be made through a namelist read from unit 5. On a Univac 1110 unit 5 is the input buffer. The namelist contained all of the parameters listed in Table II and IZEE and POT. POT is included so that specific changes to the ionization potential may be made without changing the data file on unit 12. IZEE must be chosen so that the file on unit 12 meets the conditions described in the previous paragraph. The file containing these changes must be in unit 5 and must be named INIT. An example of such a file is given in Appendix A.

There are also two types of output from this code: printed results and storage of the results on disk files. The output is achieved in subroutine OUT2. The results include Rosseland and Planck mean free paths, ionization states, and internal energies per unit mass. The mean free paths are in units

Table I
Ionization Potential Input Files

| Argon | Xenon | | |
|-------|-------|------|-------|
| 0 | 0 | 891 | 9570 |
| 15.8 | 12 | 1390 | 39300 |
| 27.6 | 21.2 | 1490 | 40300 |
| 40.7 | 31.3 | 1590 | |
| 59.8 | 42 | 1680 | |
| 75. | 53 | 1780 | |
| 91. | 58 | 1880 | |
| 124 | 135 | 1990 | |
| 143 | 143 | 2090 | |
| 422 | 171 | 2180 | |
| 478 | 202 | 2280 | |
| 539 | 233 | 2550 | |
| 618 | 264 | 2640 | |
| 686 | 294 | 2730 | |
| 756 | 325 | 2810 | |
| 855 | 358 | 3000 | |
| 918 | 389.6 | 3090 | |
| 4120 | 421 | 3300 | |
| 4430 | 452 | 3390 | |
| | 573 | 7220 | |
| | 608 | 7490 | |
| | 643 | 7760 | |
| | 678 | 8020 | |
| | 726 | 8620 | |
| | 762 | 8900 | |
| | 853 | 9330 | |

Table II
Code Controlling Parameters and Default Values

| Name | Default Value | Use |
|---------|---------------|--|
| IPRT(1) | 0 | If $\neq 0$, print absorption coefficient |
| IPRT(2) | 20 | # of steps per subintegrand |
| IPRT(3) | 0 | If $\neq 0$, print end points of subintegrations after they are sorted into numerical order |
| IPRT(4) | 0 | If $\neq 0$, print end points before they are sorted |
| DELEI | 2.D0 | Inverse of width of absorption line in eV |
| EPSL | 1.D-4 | Spacing between subintegrals |
| DELD | .5D0 | Log of the incremental ratio of densities |
| DELTR | .162995D0 | Log of the incremental ratio of radiation temperatures |
| DELTP | .162995D0 | Log of the incremental ratio of plasma temperatures |
| DLOW | 14.4314D0 | Log of lowest density in result mesh in cm^{-3} |
| TLOW | -.39794D0 | Log of lowest radiation and plasma temperatures in result mesh in eV |
| IO | 1 | Ratio of density of adjacent mesh points=DELDxIO |
| JRO | 1 | Ratio of radiation temperatures of adjacent mesh points=DELTR xJRO |
| JPO | 1 | Ratio of plasma temperatures of adjacent mesh points=DELTP xJPO |
| IMAX | 17 | # of densities in mesh |
| JRMAX | 20 | # of radiation temperatures in mesh |
| JPMAX | 20 | # of plasma temperatures in mesh |
| HIPT | 2.D4 | Largest photon energy in integration |
| HIPOT | 1.D10 | Value of POT(I) when IZEE+1 < I < 55 |

Table II (contd.)

| Name | Default Value | Use |
|-------|---------------|---|
| INOM | 11 | Mean free paths are plotted in PLOTTER for the INOM-th density |
| DENAV | 1.0E19 | The output of PREP is a subset of results grouped around a density of DENAV |
| UNFAC | 1 | The output energies are written on the disk files in units of MJ times UNFAC. |

of centimeters, the ionization states in units of electronic charge and the internal energies in units of MJ per gram times UNFAC. For each combination of density, radiation temperature and plasma temperature there is one set of these results where the density is tabulated in cm^{-3} and the temperatures are in electron volts. The printed output is exemplified in Appendix A. To be useful in other computer codes, the results are also written onto disk files. These are all written in single precision real with a 4E12.6 format, so that there are up to four numbers per record. The Rosseland mean free path is written onto unit 20, the Planck onto unit 21, the ionization state onto unit 22, and the internal energy per unit mass onto unit 23. The utility programs described in the next section may be used to plot and rearrange the data on these disk files.

Utility Programs

We have developed three utility programs to manage and plot the results of MFP. COLLECTOR and PREP arrange the results while PLOTTER draws three-dimensional plots of the results.

COLLECTOR reads the results on units 20, 21, 22 and 23 and writes them into a single file on unit 11. It is more economical to store the results on a single file so that we can conserve resources by not saving the files on units 20 through 23. Unit 11 is written with a 4E12.6 format. In this file the ionization states are written first, followed by the internal energies per unit mass. In both cases the results are written for increasing density and plasma temperature where all of the results are written for a given density before proceeding to the next higher density. The Rosseland

mean free paths and then the Planck mean free paths are written next in the file. These are written in order of increasing density, plasma temperature and radiation temperature. For each density and plasma temperature the result is written for each radiation temperature before results are written for the next plasma temperature. Once again, results are written for all plasma temperatures before results are written for a new density.

PREP reads the results stored on unit 11, selects a subset of the results and writes that subset onto unit 10. This program chooses results for ten densities centered around a value DENAV, which must be supplied by the user. If there are not more than ten densities in the results on unit 11, then this program is of no use. Unit 10 is arranged in exactly the same way as unit 11 with the exception of the number of densities chosen.

PLOTTER is a program which uses the Univac 1110 plotting software to make three-dimensional plots of the results. This program may only be used in installations where 1110 software is available. The results are read out of unit 11 and are plotted in four graphs. The Rosseland and Planck mean free paths are plotted over the plasma temperature - radiation temperature plane for a specific density. This density is the INOM-th in unit 11, where INOM is 11 unless otherwise specified by the user. The ionization states and internal energies per unit mass are plotted over the density - plasma temperature plane.

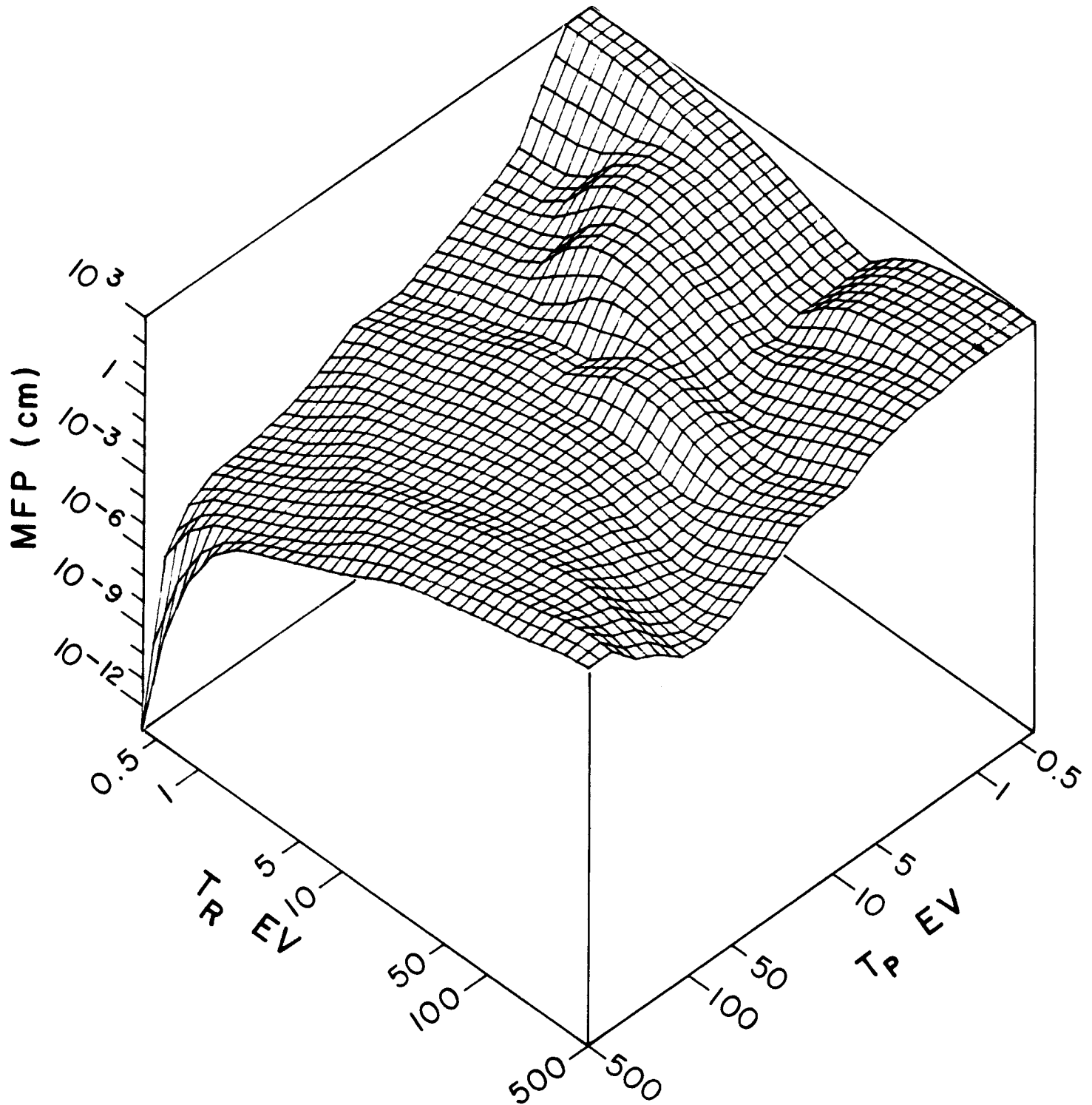
The parameters INOM and DENAV are set to the default values given in the table. Changes from these default values may be made through namelisted reads of the input file INIT, which is the file containing changes to the parameters in MFP itself.

IV. Results for Xenon and Argon

We have used MFP to calculate the Planck mean free path, the Rosseland mean free path, the ionization state and the internal energy per unit mass for xenon and argon. These results are displayed in Figs. 5 through 14. They are also stored in disk files for use in the gas response code FIRE.

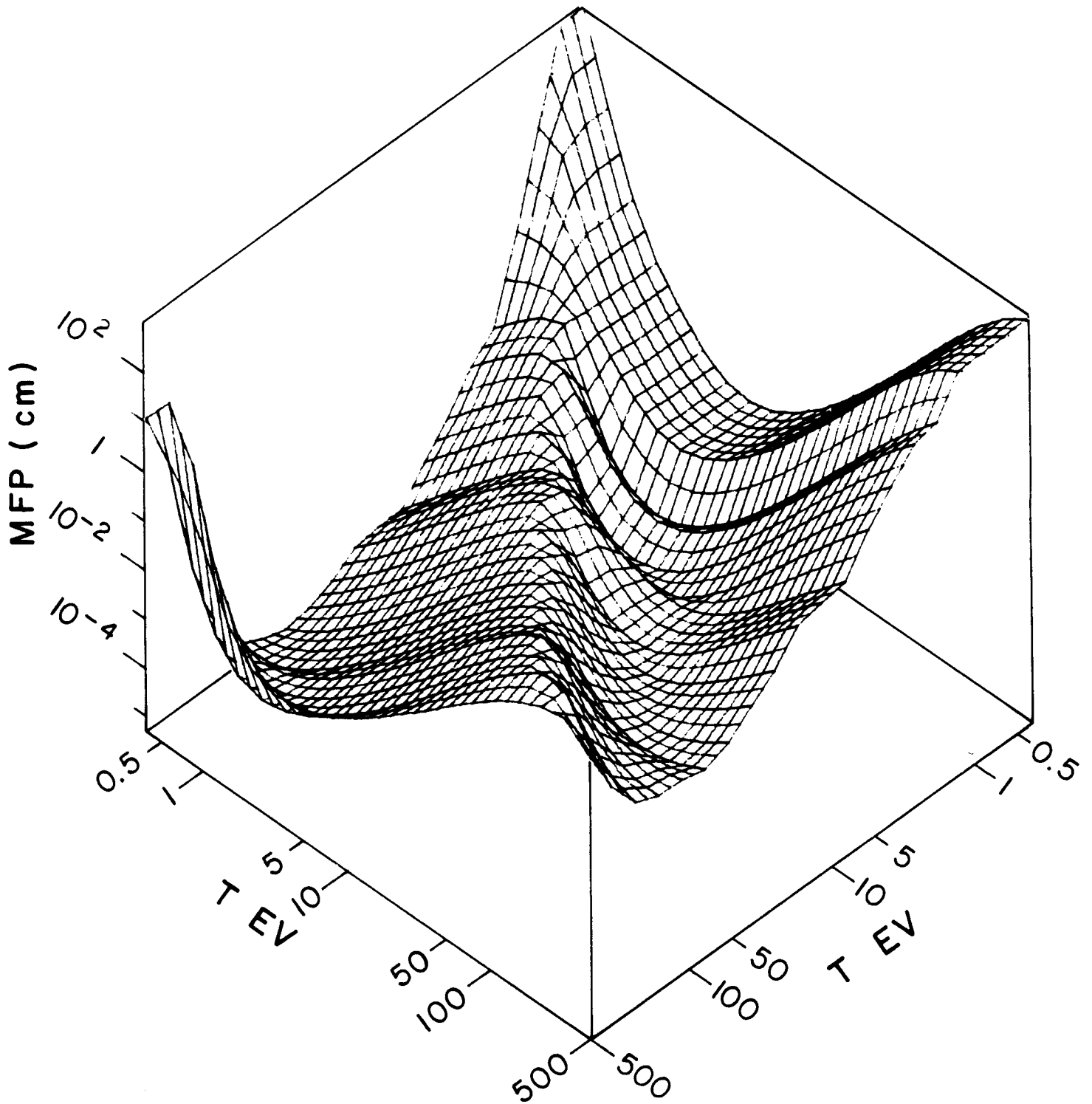
It may be noted from Figs. 5 and 6 that both mean free paths for xenon get very large at low radiation temperature and low gas temperature. As the temperature of the gas decreases, the gas becomes neutral and the atomic electrons fall into the lowest available states so that the only important photo-ionization transition becomes that which removes the ground state electron from a neutral atom. Thus, any photon which has less energy than that required to achieve this ionization will not be absorbed by the gas. For both the Rosseland and Planck mean free paths the distribution of photons in energy begins to fall below this energy as the radiation temperature drops, so that it should be expected on physical grounds that the mean free paths get large in this limit.

Fig. 7 and Fig. 8 respectively show the average ionization and the internal energy of xenon. As the gas temperature increases, so does the amount of ionization. Since the electron density also rises and since there is considerable energy stored in the ionization of the gas, the internal energy per unit mass shown in Fig. 8 is not that of an ideal gas except at low temperature, where there is little ionization.



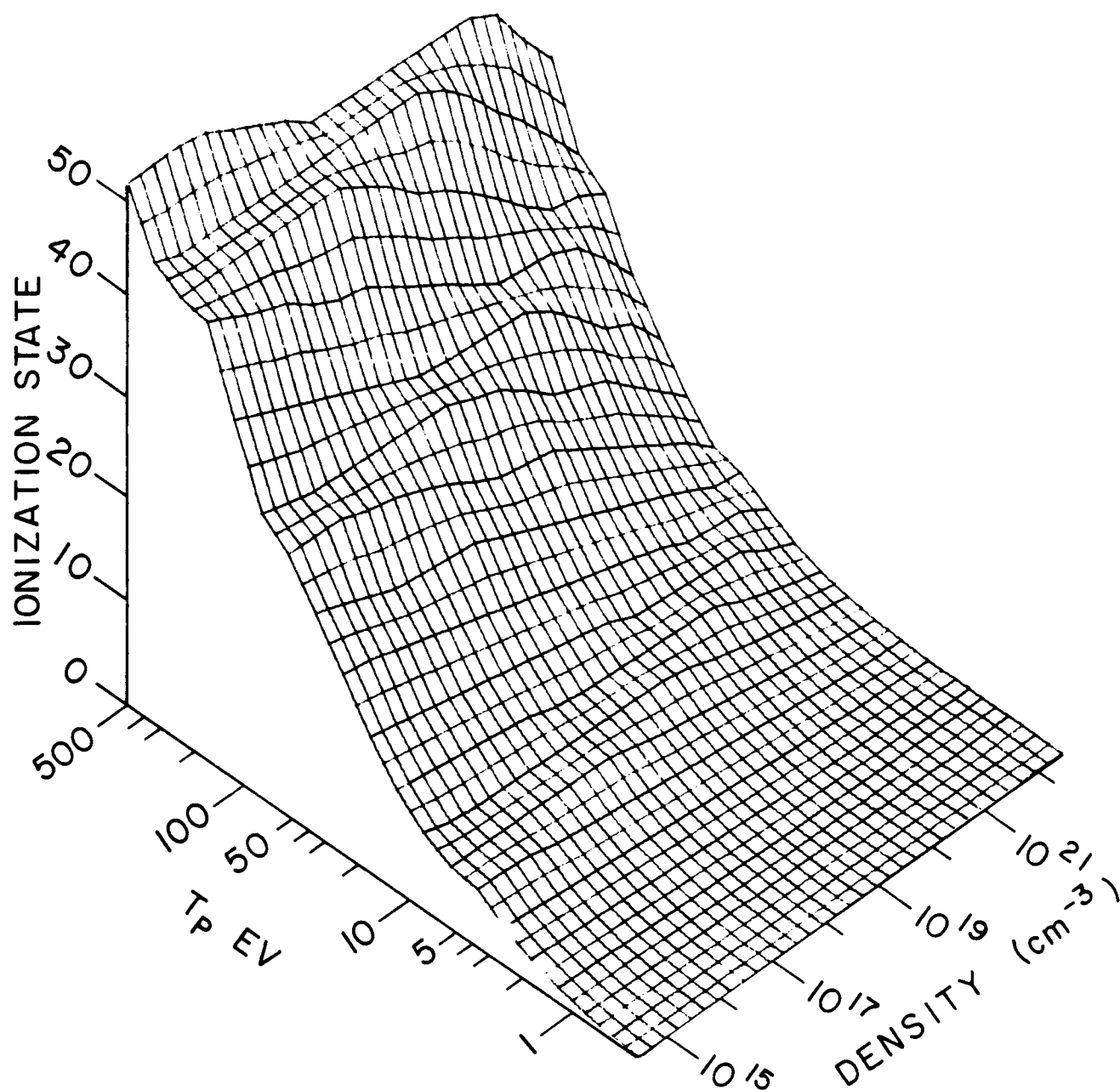
ROSSELAND MFP
 XENON DENSITY = $2.7 \times 10^{19} \text{ cm}^{-3}$

Figure 5 Rosseland mean free path for xenon at a density of $2.7 \times 10^{19} \text{ cm}^{-3}$.



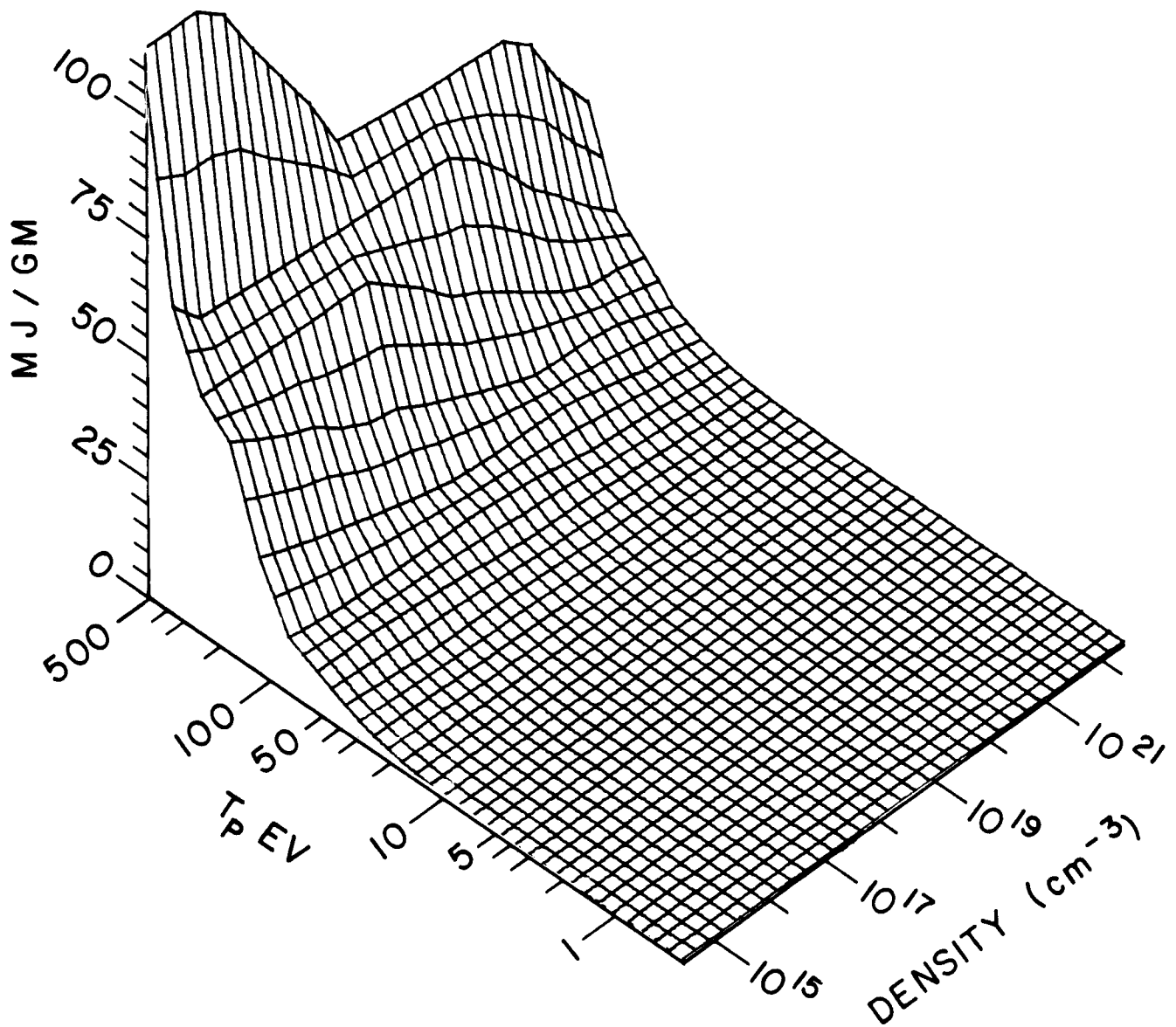
PLANCK MFP
XENON DENSITY = $2.7 \times 10^{19} \text{ cm}^{-3}$

Figure 6 Planck mean free path for xenon at a density of $2.7 \times 10^{19} \text{ cm}^{-3}$



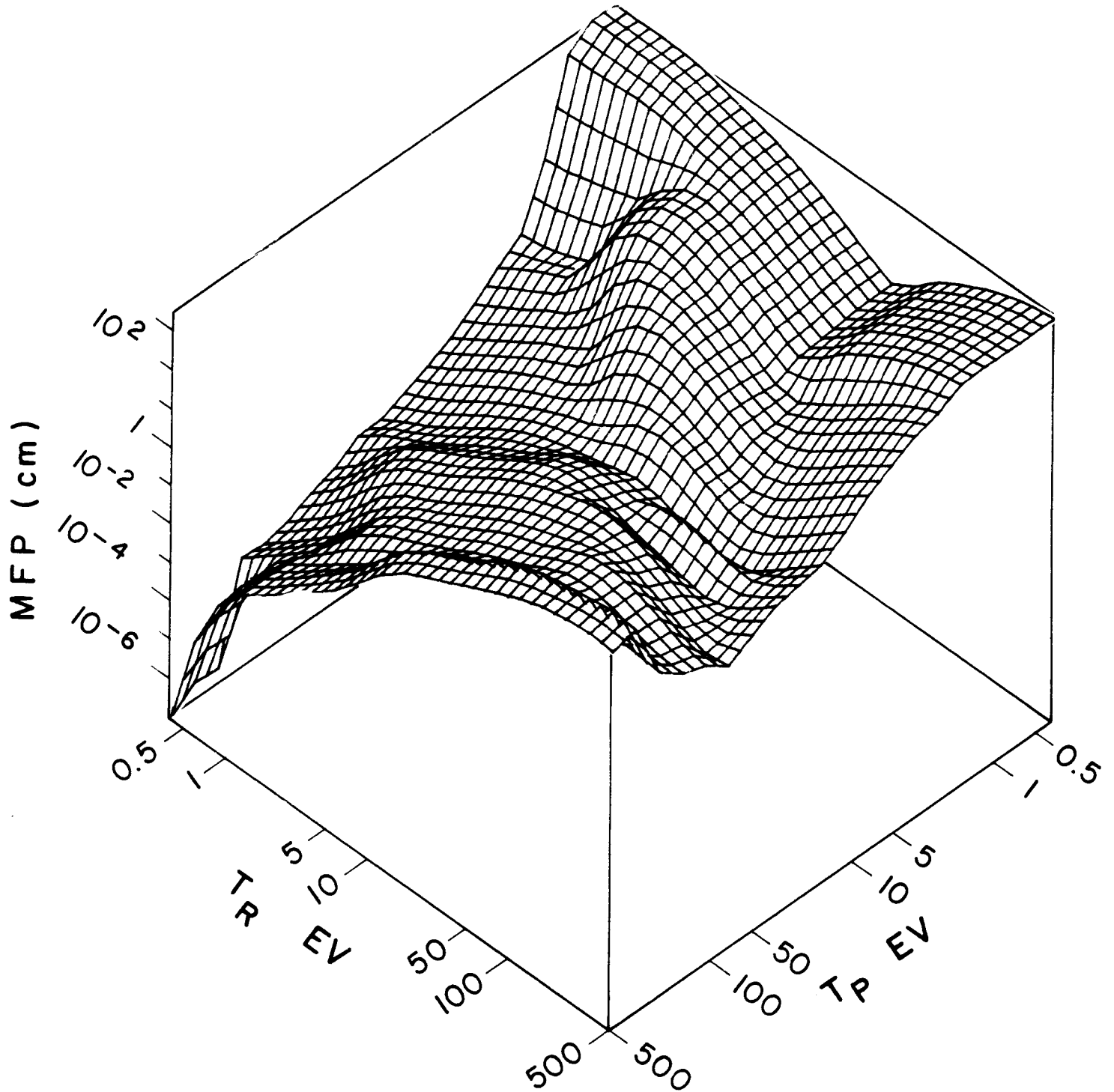
SAHA CHARGE STATE XENON

Figure 7 Average ionization state for xenon in the Saha model.



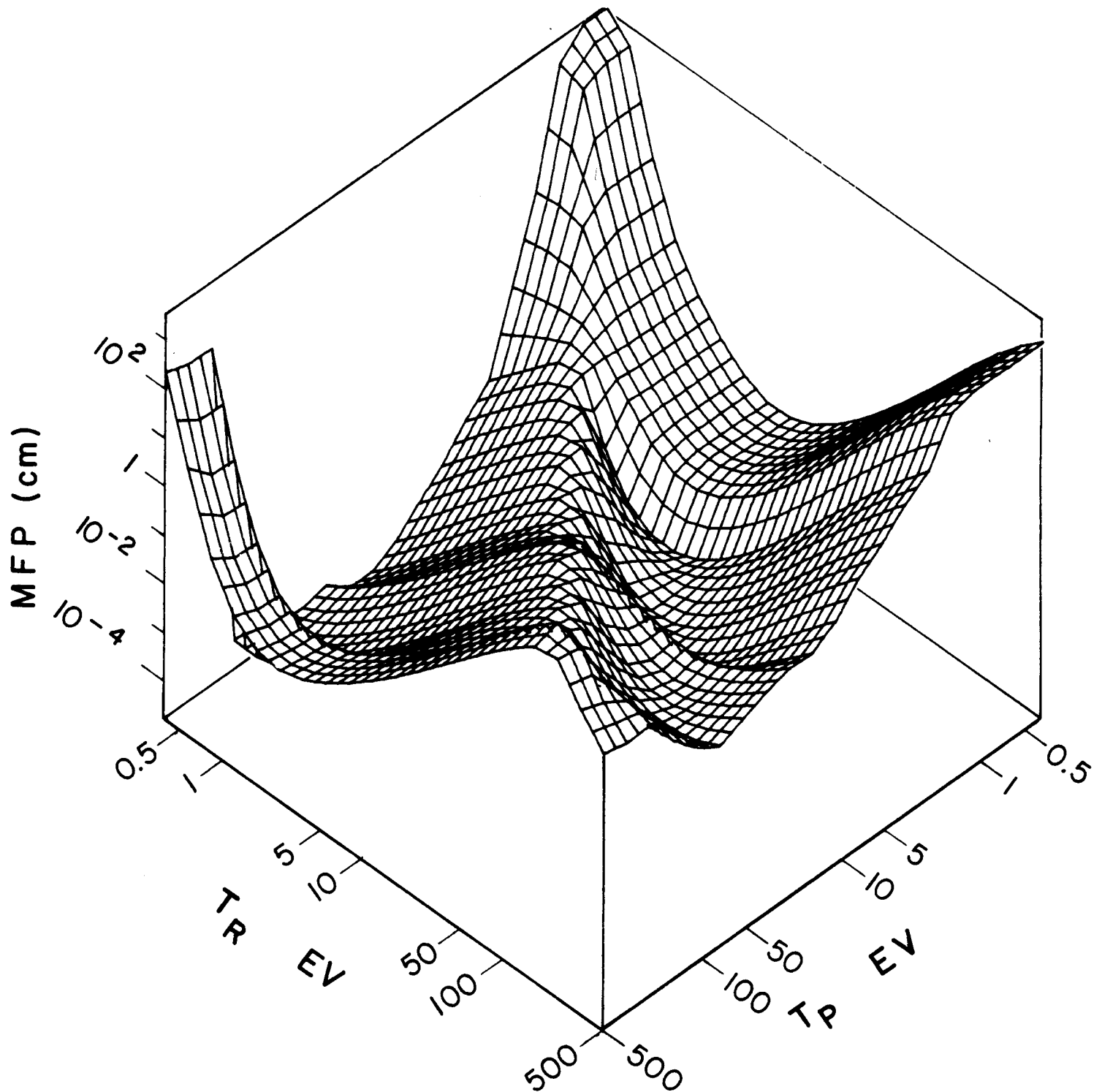
TOTAL INTERNAL ENERGY DENSITY XENON

Figure 8 Total internal energy density per unit mass for xenon.



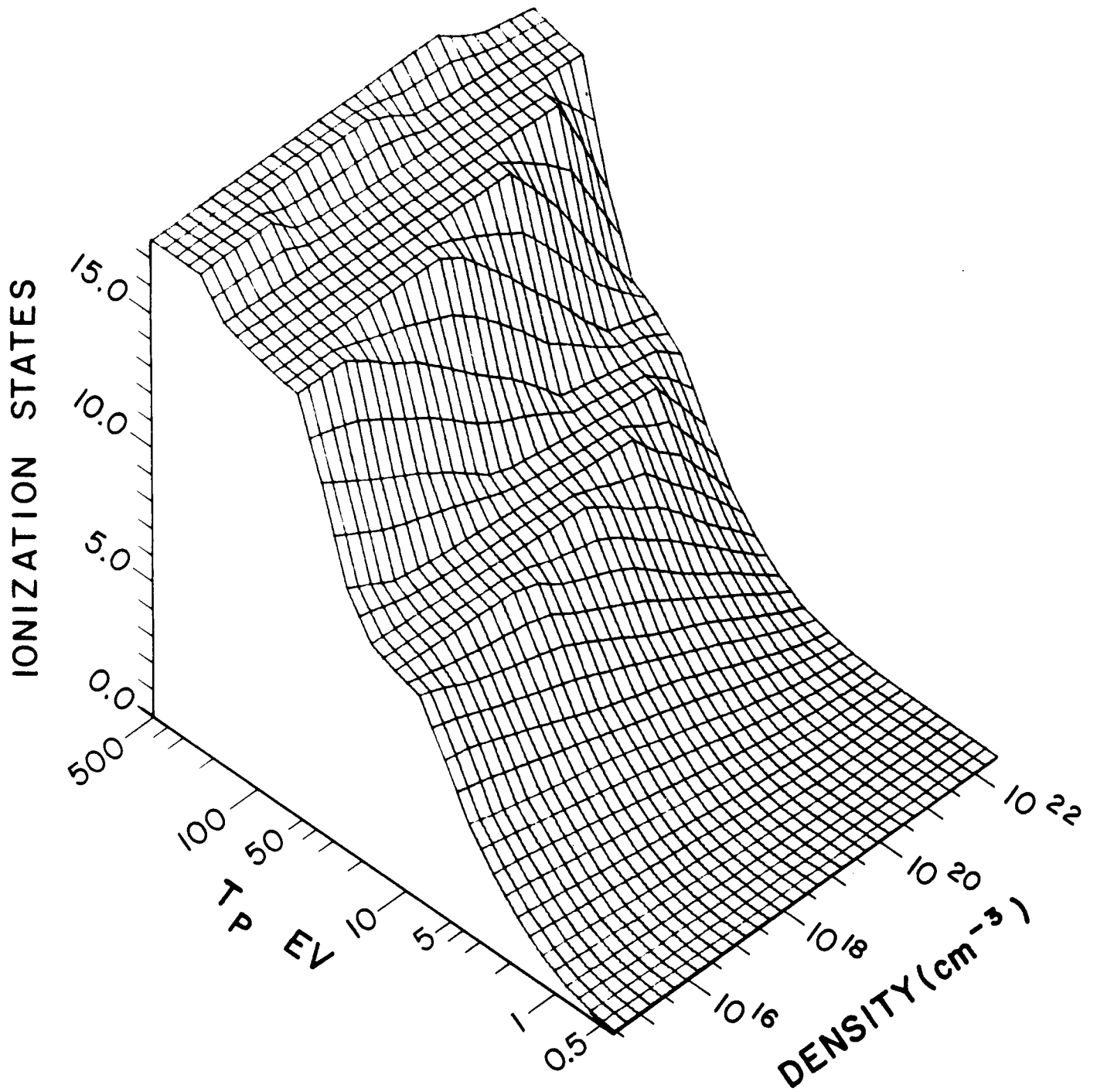
ROSSELAND MFP
 ARGON DENSITY = $2.7 \times 10^{19} \text{ cm}^{-3}$

Figure 9 Rosseland mean free path for argon at a density of $2.7 \times 10^{19} \text{ cm}^{-3}$.



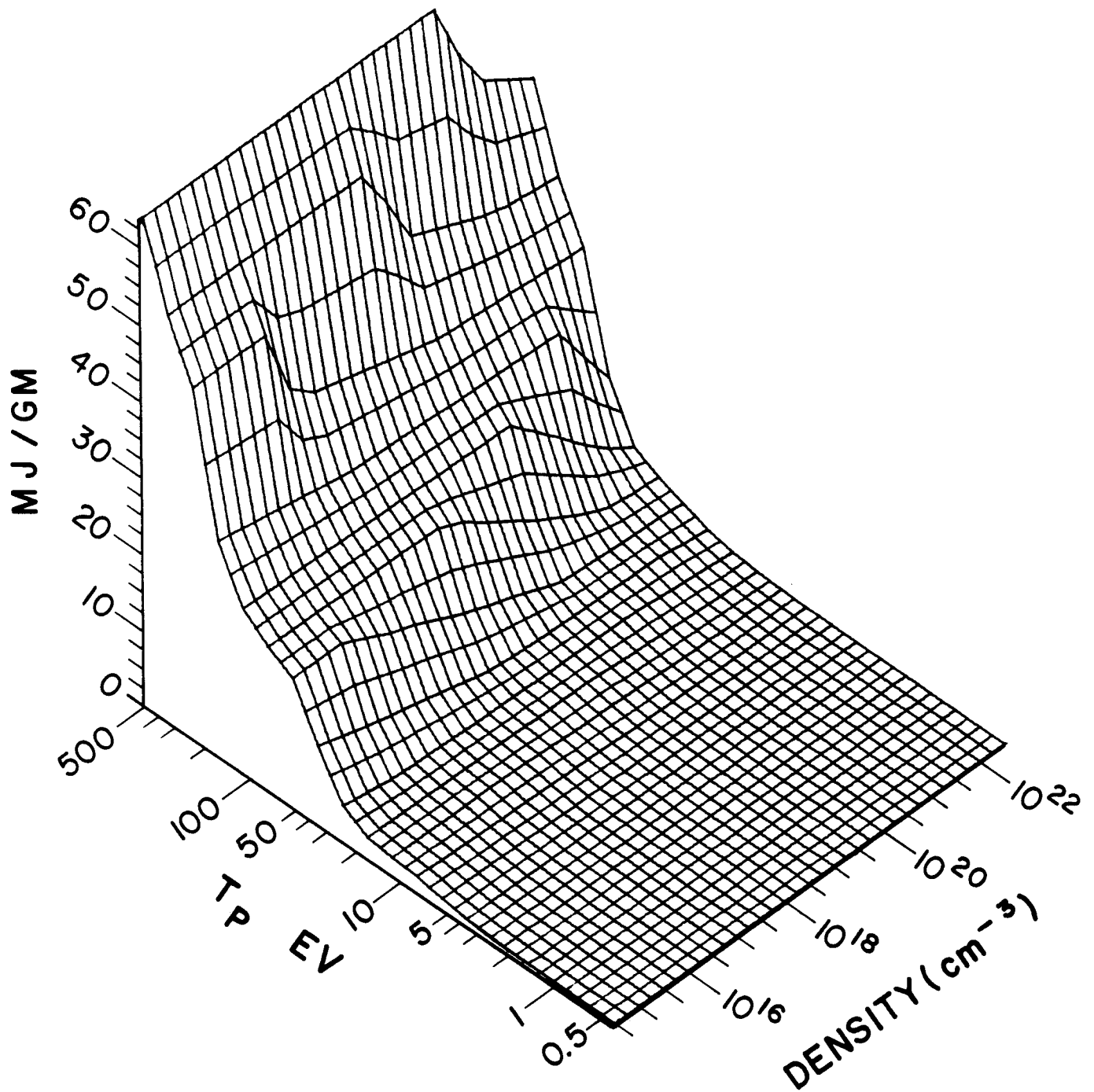
PLANCK MFP
 ARGON DENSITY $2.7 \times 10^{19} \text{ cm}^{-3}$

Figure 10 Planck mean free path for argon at a density of $2.7 \times 10^{19} \text{ cm}^{-3}$.



SAHA CHARGE STATE ARGON

Figure 11 Average ionization state for argon in the Saha model.



TOTAL INTERNAL ENERGY ARGON

Figure 12 Total internal energy density per unit mass for argon.

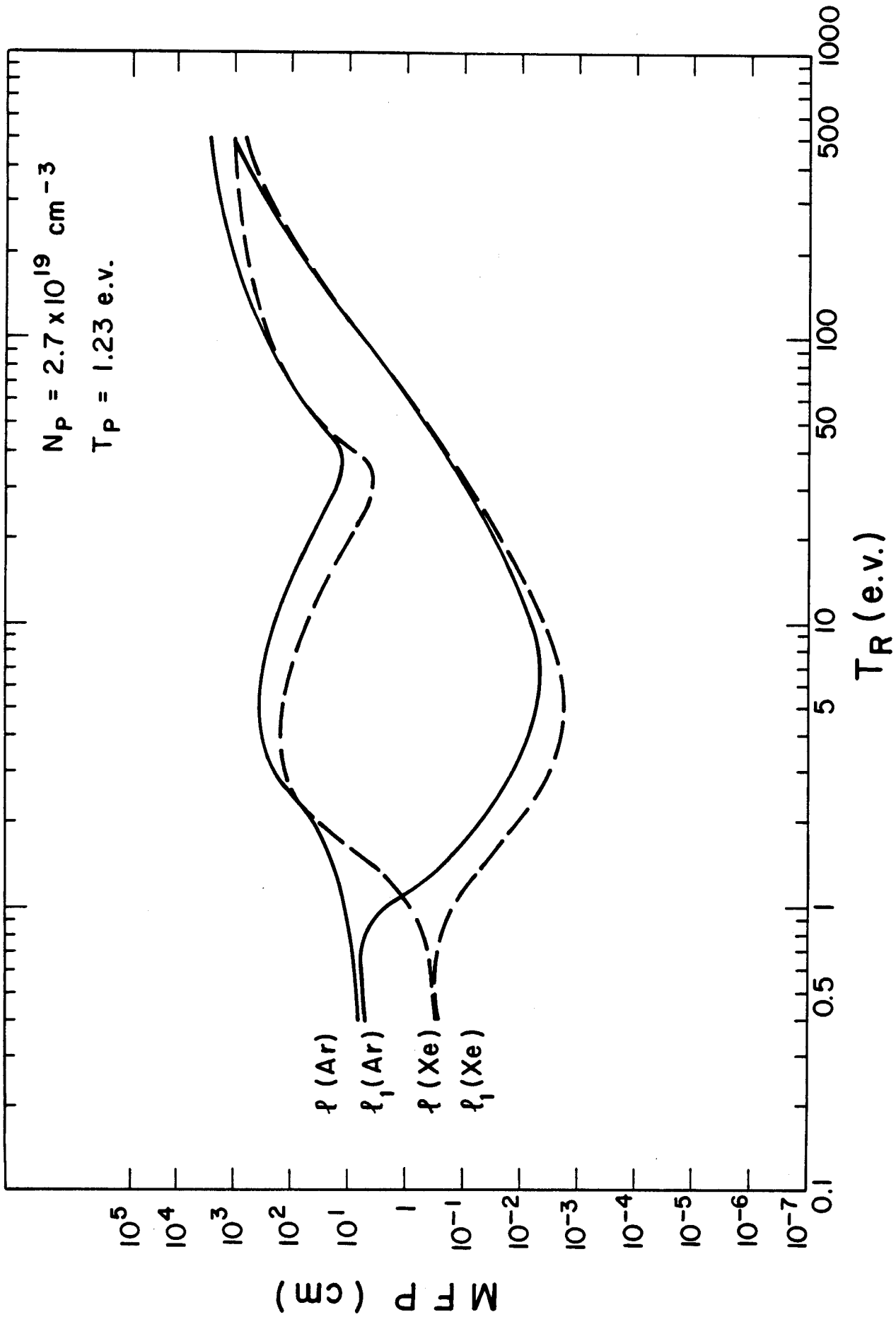


Figure 13 Comparison of Rosseland mean free paths, l , and Planck mean free paths, l_1 , for argon (solid lines) and xenon (dotted lines). The particle density is $2.7 \times 10^{19} \text{ cm}^{-3}$ and the gas temperature is 1.23 eV.

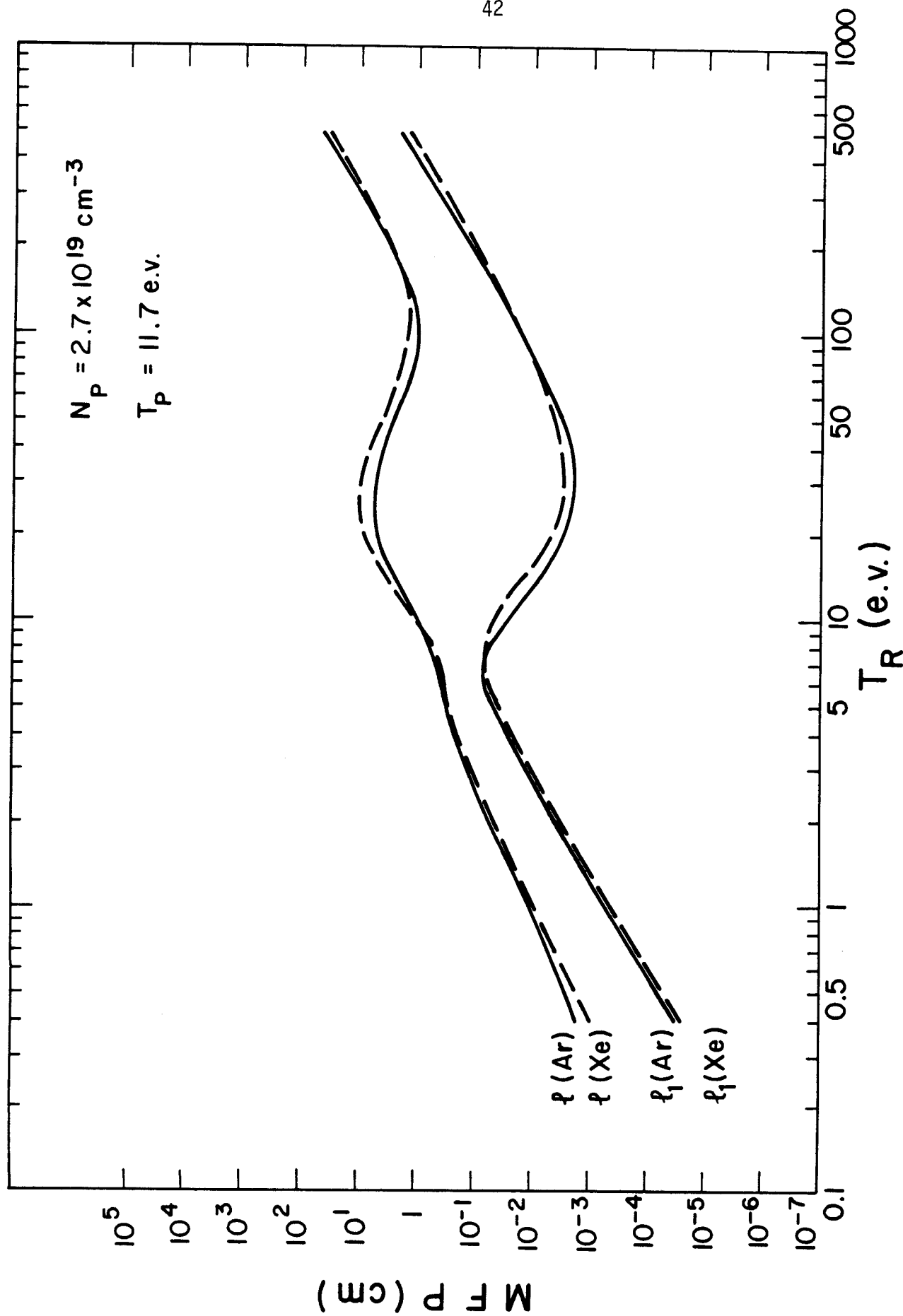


Figure 14 Comparison of Rosseland mean free paths, l , and Planck mean free paths, l_1 , for argon (solid lines) and for xenon (dotted lines). The particle density is $2.7 \times 10^{19} \text{ cm}^{-3}$ and the gas temperature is 11.7 e.v.

The results for argon are shown in Figs. 9 through 12 to be similar in character to those of xenon. Naturally, the average ionization in Fig. 10 can be no larger than 18 for argon. In Figs. 13 and 14, the mean free paths for the two gases are compared at atmospheric density for gas temperatures of 1.23 eV and 11.7 eV, respectively. In both cases the Planck mean free paths become larger than the Rosseland mean free paths only at large radiation temperatures. It is interesting to note that, when the gas temperature is 1.23 eV, the choice of gas species makes no significant difference for radiation temperatures above 20 eV. This occurs because the ionization of the gases is low enough that the absorption spectrum is as in Fig. 3 so that the absorption of large energy photons is the same for both gases; for low energy photons, the dissimilarities in the ionization energies cause the absorption to be different. In the case pictured in Fig. 14, where the gas temperature is 11.7 eV, there is enough ionization and atomic excitation of the gases that the absorption coefficients have several important peaks at large energies. The absorption of photons with energies up to 500 eV then becomes dependent upon the ionization potentials of the gases.

V. Conclusions and Recommendations

This study provides data necessary for the computer simulation of the propagation of a pellet micro-explosion generated fireball through a gas. These parameters, based on an admittedly simple physical model, have been displayed and stored for use in an ion beam fusion study. We feel that the computer

code and the results presented here are very important to a study of fire-ball propagation in that we have gained flexibility in the species, density and temperature of the background gases chosen. Additionally, we have gained the ability to allow nonequilibrium between the gas and the radiation because we now have radiation transport parameters for the case when the radiation and gas temperatures are dissimilar.

There are some improvements that we may make to this study. The treatments of the four mechanisms of radiation absorption may be improved upon by using more sophisticated physical models. One such change that could have a significant effect is using the impact approximation to calculate the atomic line widths. Additionally, the coronal model for gas ionization may be included for low density high temperature gases. However, this work is always limited by the data available for the ionization energies of the gas considered, so that improving the calculation may not be justified for xenon, for example, where the atomic data is still largely undecided. The data is much better for argon so that these improvements may be justified.

Acknowledgement

This work was supported by Sandia Laboratory, Albuquerque, NM, under contract to the United States Department of Energy.

References

1. R.W. Conn, et al., "SOLASE, A Laser Fusion Reactor Study", Univ. of Wisconsin, Nuclear Engineering Department Report UWFD-220 (Dec. 1977), Chapters X and XI.
2. Ya. B. Zel'dovich and Yu. P. Raizer, Physics of Shock Waves and High-Temperature Hydrodynamic Phenomena (Academic Press, New York, 1967), page 519.
3. Ibid, Chapter V.
4. Ibid, Chapter III.
5. D.L. Miller and J.D. Dow, Phys. Lett. 60A, 16 (1977).
6. D.L. Miller, J.D. Dow, R.G. Houlgate, G.V. Marr, and J.B. West. J. Phys. B: Atom. Molec. Phys. 10, 3205 (1977).
7. J.L. Franklin, J.G. Dillard, H.M. Rosenstock, J.T. Herron, and K. Draxl, Nat. Stand. Ref. Data Ser., Nat. Bus. Stand. (U.S.), 26 (June 1969).
8. T.A. Carlson, C.W. Nestor, Jr., N. Wasserman, and J.D. McDowell, Atomic Data, 2, 63 (1970).
9. D. Mosher, NRL Memorandum Report 2563 (March 1973).
10. J.D. Jackson, Classical Electrodynamics (John Wiley & Sons, Inc., New York, 1962), page 490.
11. H.A. Bethe and E.E. Salpeter, Quantum Mechanics of One- and Two-Electron Atoms (Academic Press, Inc., New York, 1957), page 313.
12. L.M. Biberman and A.N. Lagarkov, Opt. Spectr. (USSR) (English Transl.), 16, 173 (1964).
13. M. Baranger, Atomic and Molecular Processes (Academic Press, Inc., New York, 1962), D.R. Bates, ed., pages 493-548.
14. Ya. B. Zel'dovich and Yu. P. Raizer, Physics of Shock Waves and High-Temperature Hydrodynamic Phenomena (Academic Press, New York, 1967), Chapter II.

Appendix A

We now present an example of the use of MFP. The problem shown is for argon at a density of 1.67×10^{18} and for gas temperatures of .4 eV and .58 eV. Only the first ten default radiation temperatures are used so that the input namelist, which is held in element MFP•INIT and is called INIT, becomes

MFP•INIT

```
&INIT IZEE=18,  
      ATMAS=6.666D-23,  
      DELEI=.2D0,  
      IMAX=1,  
      JPMAX=2,  
      JRMAX=10,  
      DLOW=18.2227D0  
&END
```

The first page of output is the heading shown on the next page. This page is printed by subroutine INPUT and it lists all of the parameters used in MFP. The energies EPSL, HIPT, HIPOT and 1/DELEI as well as the temperatures TLOW, DELTR and DELTP are all in units of eV. The densities DLOW and DELD are in cm^{-3} and the mass ATMAS is in grams.

```

*****
*
*      MFP - A CODE TO CALCULATE THE
*      EQUATIONS OF STATE AND OPACITIES
*      OF NOBLE GASES
*
*      WRITTEN BY ROBERT R. PETERSON
*
*****

```

IPRT(I)

```

IPRT(1)= 0      PRINT ABSORPTION COEF?
IPRT(2)= 20     # STEPS / SUBINTEGRAND
IPRT(3)= 0      PRINT ENDPOINTS AFTER SORT?
IPRT(4)= 0      PRINT ENDPOINTS BEFORE SORT?

```

CONSTANTS USED

```

DELEI= .200000+000      WIDTH OF ABS. LINE
EPSL= .100000-003      SPACE BETWEEN INTEGRALS
HIPT= .200000+005      HIGHEST PHOTON ENERGY
HIPOT= .100000+011      DEFAULT IONIZATION POT
IZEE= 18                ATOMIC #
ATMAS= .666600-022      MASS OF ATOM
UNFAC= .100000+001      MJ PER ENERGY UNIT

```

CONSTANTS FOR RESULT MESH

```

IMAX= 1                # OF DENSITIES
JRMAX= 10              # OF RAD TEMPS
JPMAX= 2               # OF GAS TEMPS
DLOW= .182227+002      LOG OF LOWEST DENSITY
TLOW= -.397940+000     LOG OF LOWEST TEMPS
DELTR= .162995+000     LOG OF RATIO OF SUCCEEDING RAD TEMPS
DELTP= .162995+000     LOG OF RATIO OF SUCCEEDING GAS TEMPS
DELD= .500000+000      LOG OF RATIO OF SECCEEDING DENSITIES
IO= 1                  DENSITY SKIP FACTOR
JRO= 1                 RAD TEMP SKIP FACTOR
JPO= 1                 GAS TEMP SKIP FACTOR

```

The remaining page(s) of output are generated by the subroutine OUT2 and is shown below for this example. The units are clearly marked - the density is in cm^{-3} , the temperatures are in eV, the mean free paths are in cm, the ionization state is in units of electronic charge and the energy density is in MJ/gm. Even though the energy densities written on the disk files are in MJ/gm times UNFAC, the printed results remain in MJ/gm.

DENSITY= .166994+19 /CM**3

| DENSITY /CM**3 | RAD TEMP E.V. | GAS TEMP E.V. | ROSS MFP CM | THIN MFP CM | CHARGE E | ENERGY DENS MJ/GM |
|-------------------|------------------|------------------|----------------|----------------|-------------|----------------------|
| .166994+19 | .400000+00 | .400000+00 | .527895+05 | .541060+05 | .240654-U5 | .144204-02 |
| .166994+19 | .582177+00 | .400000+00 | .528006+05 | .188422+05 | .240654-U5 | .144204-02 |
| .166994+19 | .847325+00 | .400000+00 | .526902+05 | .194421+03 | .240654-U5 | .144204-02 |
| .166994+19 | .123323+01 | .400000+00 | .505767+05 | .872172+01 | .240654-U5 | .144204-02 |
| .166994+19 | .179490+01 | .400000+00 | .416264+05 | .134679+01 | .240654-U5 | .144204-02 |
| .166994+19 | .261237+01 | .400000+00 | .281043+05 | .387898+00 | .240654-U5 | .144204-02 |
| .166994+19 | .380216+01 | .400000+00 | .186418+05 | .144777+00 | .240654-U5 | .144204-02 |
| .166994+19 | .553382+01 | .400000+00 | .125591+05 | .864187-01 | .240654-U5 | .144204-02 |
| .166994+19 | .805416+01 | .400000+00 | .724302+04 | .888105-01 | .240654-U5 | .144204-02 |
| .166994+19 | .117224+02 | .400000+00 | .353903+04 | .141351+00 | .240654-U5 | .144204-02 |

| DENSITY /CM**3 | RAD TEMP E.V. | GAS TEMP E.V. | ROSS MFP CM | THIN MFP CM | CHARGE E | ENERGY DENS MJ/GM |
|-------------------|------------------|------------------|----------------|----------------|-------------|----------------------|
| .166994+19 | .400000+00 | .582177+00 | .527537+05 | .540735+05 | .193787-U2 | .217632-02 |
| .166994+19 | .582177+00 | .582177+00 | .527452+05 | .188367+05 | .193787-U2 | .217632-02 |
| .166994+19 | .847325+00 | .582177+00 | .526173+05 | .194420+03 | .193787-U2 | .217632-02 |
| .166994+19 | .123323+01 | .582177+00 | .505108+05 | .872172+01 | .193787-U2 | .217632-02 |
| .166994+19 | .179490+01 | .582177+00 | .415818+05 | .134679+01 | .193787-U2 | .217632-02 |
| .166994+19 | .261237+01 | .582177+00 | .280799+05 | .387898+00 | .193787-U2 | .217632-02 |
| .166994+19 | .380216+01 | .582177+00 | .186302+05 | .144777+00 | .193787-U2 | .217632-02 |
| .166994+19 | .553382+01 | .582177+00 | .125540+05 | .864187-01 | .193787-U2 | .217632-02 |
| .166994+19 | .805416+01 | .582177+00 | .724080+04 | .888105-01 | .193787-U2 | .217632-02 |
| .166994+19 | .117224+02 | .582177+00 | .353805+04 | .141351+00 | .193787-U2 | .217632-02 |

@PDG,N .S, RESTORE STANDARD PAPER